JOURNAL OF AIRCRAFT
Vol. 42, No. 6, November–December 2005

Engineering Notes

ENGINEERING NOTES are short manuscripts describing new developments or important results of a preliminary nature. These Notes should not exceed 2500 words (where a figure or table counts as 200 words). Following informal review by the Editors, they may be published within a few months of the date of receipt. Style requirements are the same as for regular contributions (see inside back cover).

Aerodynamic Characteristics of an Elliptic Airfoil at Low Reynolds Number

Kijung Kwon*
Korea Aerospace Research Institute, Daejeon 305-333, Republic of Korea
and
Seung O. Park†
Korea Advanced Institute of Science and Technology, Daejeon 305-701, Republic of Korea

Introduction

RECENTLY unmanned vertical takeoff and landing vehicles have attracted aeronautical engineers' attention. One of those is a canard rotor/wing (CRW) aircraft, and several studies have been reported.[1–3] CRW aircraft usually employs a two-bladed rotor to takeoff the ground; after taking off, it locks the rotor to act as a fixed wing, allowing it to cruise at high speed. This requires that the cross section of the rotor blades be elliptic.

Flow past an elliptic cylinder or ellipse cross-sectioned airfoil has been studied for a long time because of its significance in fundamental flow physics and its practical importance. However, most studies so far have been concerned with unsteady flow characteristics and/or heat transfer at very low Reynolds numbers. Aerodynamic characteristics such as lift, drag, and pitching moment variations with angle of attack have rarely been reported. Zahm et al.[4] reported the drag and surface pressures of four elliptic cylinders of different thickness ratio for various yaw angles. Schubauer[5] carried out an intensive study of the boundary layer around an elliptic cylinder. This study, however, focused on the relationship between the boundary-layer transition and the freestream turbulence intensities for a 33.8% thickness elliptic cylinder at zero angle of attack. Hoerner and Borst[6] reported lift coefficients of elliptic airfoils having various thickness ratios for the Reynolds numbers of 2×10^6 and 7×10^6. White[7] compiled the drag coefficients of several elliptic cylinders with various thicknesses for zero angle of attack in laminar and turbulent flow conditions.

Wings for unmanned vehicles are often operated at low Reynolds number. At such low Reynolds numbers, aerodynamic characteristics can be dominated by laminar flow phenomena including transition and separation bubbles. Gleyzes et al.[8] reported boundary-layer profiles of an elliptic airfoil at a very high angle of attack. Lang et al.[9] successfully used a particle image velocimetry (PIV) technique to investigate the transition in the boundary layer of an artificially generated separation bubble.

The primary objective of the current work is to investigate aerodynamic characteristics of a 16% thickness elliptic airfoil at the Reynolds number of 3×10^5. Measurements were taken for the airfoil with and without a boundary-layer transition trip.

Experiment

Tests were conducted in a low-speed wind tunnel at Korea Aerospace Research Institute. The wind tunnel is a closed-circuit type and has the test section size of 1 m width, 0.75 m height, and 2 m length. The maximum achievable wind speed is 110 m/s, and the turbulence intensities for the case of empty test section are 0.12% in streamwise direction and 0.15% in vertical and lateral directions. The static pressure gradient along the tunnel axis is below 0.03 %/m.

The cross-sectional shape of the airfoil of the present study was an ellipse whose major axis, the chord length, was 200 mm and the minor axis 32 mm. The span of the model was 990 mm, yielding an aspect ratio of 4.95. The Reynolds number based on the chord was 3×10^5 with the freestream velocity of about 25 m/s. On the upper and lower surfaces of the airfoil, 25 pressure holes were placed on each side. The spacing between the pressure taps was chosen to be approximately proportional to the local curvature, which made the minimum spacing 1.7 mm and the maximum 28.8 mm.

Tests were performed with and without a boundary-layer transition trip attached on the 10% chord from the leading edge on both sides of the airfoil surface. Circular trip dots with the spacing of 1.27 mm were made of vinyl tape and the dot Reynolds number was about 435. The diameter of the dots was 1.27 mm and the height 0.29 mm.

Lift and Drag Measurements

Sectional lift was obtained by integrating the pressure distribution. The surface pressures were measured with a pressure scanner from Scanivalve Corporation (ZOC) equipped with pressure transducers of 1 psi differential range. Sectional drag coefficient was determined from the wake survey by using a rake located at the three-chord downstream station from the trailing edge. Wake measurements were taken across ±186 mm width both above and below the chord line at zero angle of attack. To check the spanwise nonuniformity of the wake, measurements were conducted at midspan and at ±70-mm from the mid-span spanwise stations. The rake consisted of 47 total pressure probes whose inner and outer diameters were 0.6 and 1.6 mm, respectively and 3 pitot-static probes. One pitot-static probe was positioned at the wake center, and the other two were located at a position ±66 mm from the wake center. Lift, pitching moment, and drag coefficients as well as angles of attack were corrected to account for the effects of solid blockage, wake blockage, and streamline curvature as described in Ref. 10. We adopted Thom's solid blockage and Maskell's wake blockage methods.

Uncertainties

Uncertainty estimates of various measurements of the present work were carried out following AIAA standard S-071A-1999.[11] The uncertainties of the lift coefficients were found to lie between 0.0124 at $\alpha = 0$ deg and 0.0145 at $\alpha = 12$ deg. The pitching moment

Received 21 March 2005; presented as Paper 2005-4762 at the AIAA 23rd Applied Aerodynamics Conference, Toronto, Canada, 6–10 June 2005; revision received 27 June 2005; accepted for publication 28 June 2005.

*Senior Researcher, Aerodynamics Department, 45 Eoeun-dong, Yuseong-gu. Member AIAA.
†Professor, Department of Aerospace Engineering, 373-1 Kusong-dong, Yuseong-gu. Senior Member AIAA.

coefficient and the drag coefficient uncertainties were estimated to be 0.001 and 0.0023, respectively. The uncertainties of the pressure coefficients at each pressure tap had different values for different angles of attack. The uncertainty of the pressure coefficient at $x/c = 0.04$, for example, had the largest uncertainty, 0.052, at $\alpha = 11$ deg. However, the pressure coefficients over the surface behind the quarter-chord point were found to have rather constant uncertainty estimates of around 0.038.

Experimental Results

Lift Coefficients and Pressure Distributions

Figure 1 shows the C_l curves for both the smooth and the tripped airfoils. Also included is the C_l curve from Hoerner and Borst.[6] The discrepancy between the present curve and the Ref. 6 results must be due to the enormous Reynolds number difference: 3×10^5 for the present test and 2×10^6 for the Ref. 6 case. This demonstrates that the lift of the present elliptic airfoil is very dependent on the Reynolds number, which is rather unusual for conventional airfoils. For the range from $\alpha = 0$-4 deg, the lift curve slopes $C_{l\alpha}$ of the smooth and the tripped cases remain fairly constant, although the slopes are different from each other. The slopes are about 3.17π and 1.83π for the smooth and the tripped cases, respectively. When the angle of attack exceeds 6 deg, C_l for both cases behaves similarly, and $C_{l\max}$ of about 1.1 is reached at $\alpha = 11$ deg.

A value of lift curve slope much greater than 2π is very unusual compared to the case of conventional airfoils. From the pressure distributions (Fig. 2) and the near-wake streamline patterns drawn from the PIV measurements given in Ref. 12, we found that an asymmetric flow separation around the trailing edge of the smooth airfoil was the cause of this high lift curve slope at low angles of attack. From the fact that the two C_l curves of the present study merge beyond $\alpha = 6$ deg, we conjecture that the trip effect disappears beyond this angle of attack. This signifies that transition takes place over the airfoil surface for the case of smooth airfoil.

Figure 2 shows variation of the pressure coefficient distributions C_p for several angles of attack. At $\alpha = 0$ deg, the pressure distributions for the smooth and tripped cases are about the same except for the region near the trailing edge. This is due to the difference in the separation pattern near the trailing edge. Obviously, the separation region is larger for the smooth airfoil. As the angle of attack increases, the difference in the pressure distributions for the two cases becomes greater, as seen in the pressure distributions for $\alpha = 2$ and 4 deg. At $\alpha = 4$ deg, we see that the pressure of the smooth airfoil is much less on the suction side and much greater on the pressure side. This makes the lift coefficient of the smooth airfoil much larger than that of the tripped airfoil at low angles of attack as shown in Fig. 1. When the angle of attack exceeds 6 deg, the pressure distributions do not differ much between the smooth and the tripped cases.

Note that the difference between the pressure distributions at $\alpha = 2$ and 4 deg looks similar to the change of pressure distribution for a case of a flapped airfoil. For an airfoil with deflected flap, the pressure distribution curve over the upper surface of the main wing moves upward and that over the lower surface moves downward. From the PIV measurement data given in Ref. 11, we found that these different pressure distributions were mainly due to the separation bubble and its vortex strength near the trailing edge. For the case of the smooth airfoil, the boundary layer separated earlier and the separation bubble was significantly larger.

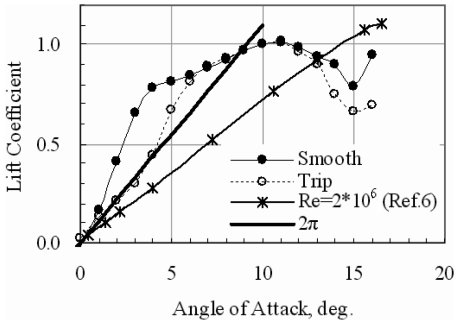

Fig. 1 Lift coefficients with respect to angle of attack.

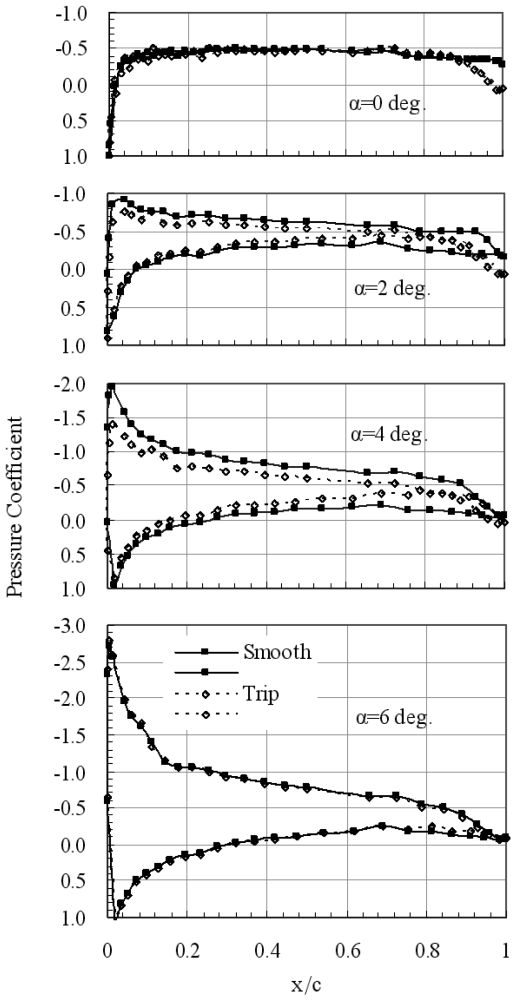

Fig. 2 Surface pressure distributions at various angles of attack.

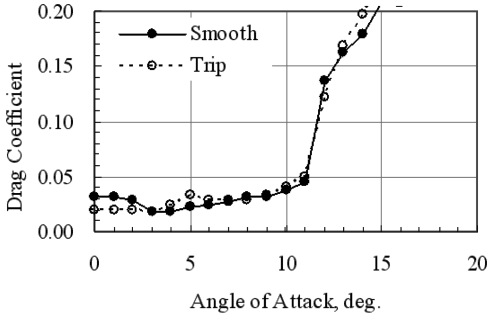

Fig. 3 Drag coefficients.

Drag and Pitching Moment Coefficients

Figure 3 shows the drag coefficient variations with angle of attack. We find that the drag coefficient of the smooth airfoil is greater than that of the tripped airfoil when the angle of attack is below 4 deg. This is obviously due to the flow separation. The minimum C_d is about 0.018 for the smooth airfoil at $\alpha = 4$ deg and about 0.019 for the tripped airfoil at $\alpha = 0$ deg. As the angle of attack increases above $\alpha = 11$ deg where $C_{l\max}$ is obtained, C_d increases abruptly reflecting that the airfoil is in stall.

Figure 4 shows the variation of the pitching moment coefficient about the quarter-chord, $C_{m/4}$. In contrast to conventional airfoils, which have nearly constant $C_{m/4}$ in the linear range, the pitching moment of the present case is seen to vary irregularly with the angle

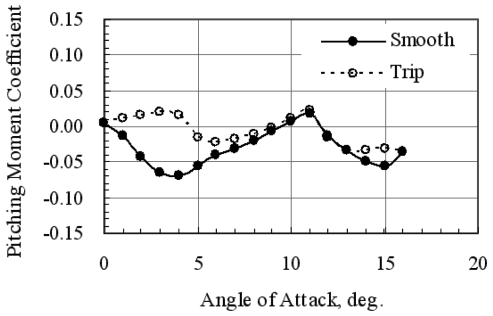

Fig. 4 Pitching moment coefficients.

of attack. For the case of symmetric airfoil, such as NACA0012, $C_{m/4}$ is nearly zero in the linear range (Ref. 13). For the case of the tripped airfoil, the variation of $C_{m/4}$ below the stall angle is not so severe as that for the smooth airfoil, with the mean value being approximately zero. For the smooth airfoil, the pressure distributions seen in Fig. 2 ($\alpha = 2$ and 4 deg), especially those behind the quarter-chord point, contribute to generate nose-down pitching moment. This causes the pitching moment coefficient to become negative, as seen in Fig. 4. This is qualitatively similar to the fact that the flap deflection increases the lift and decreases the pitching moment.

Conclusions

Aerodynamic characteristics of a 16% thickness elliptic airfoil at the Reynolds number of 3×10^5 were studied experimentally, and we found that they were very different from those of conventional airfoils. Experiments were conducted for two flow conditions: one for the smooth airfoil and the other for the airfoil with a transition trip. When the angle of attack was below 4 deg, the lift curve slope for the smooth airfoil was much greater than 2π, whereas that for the tripped airfoil was about 2π. Beyond the angle of attack of 6 deg, the effect of trip was found to disappear. This large lift coefficient, when compared with conventional symmetric airfoils, was caused by the presence of asymmetric separation bubbles near the trailing edge. The pitching moment coefficients about the quarter-chord were found to vary significantly with the angle of attack in great contrast to those of conventional airfoils.

Acknowledgments

This study was supported by the Korea Research Council of Public Science and Technology. Partial support also came from the BK-21 project from the Ministry of Education.

References

[1]Rutherford, J. W., Bass, S. M., and Larsen, S. D., "Canard Rotor/Wing: A Revolutionary High-Speed Rotorcraft Concept," AIAA Paper 93-1175, Feb. 1993.

[2]Thompson, T. L., Smith, R. L., Helwani, M., Shockey, G. A., and Schwimley, S. L., "Wind Tunnel Test Results for a Canard Rotor/Wing Aircraft Configuration," *Proceedings of the American Helicopter Society 57th Annual Forum*, American Helicopter Society, Alexandria, VA, 2001.

[3]Pandya, S. A., and Aftosmis, M. J., "Computation of External Aerodynamics for a Canard Rotor/Wing Aircraft," AIAA Paper 2001-0997, Jan. 2001.

[4]Zahm, A. F., Smith, R. H., and Louden, F. A., "Forces on Elliptic Cylinders in Uniform Air Stream," NACA Rept. 289, NACA TR-315, 1929.

[5]Schubauer, G. B., "Air Flow in the Boundary Layer on an Elliptic Cylinder," NACA Rept. 652, 1939.

[6]Hoerner, S. F., and Borst, H. V., "Lift Characteristics of Foil Sections," *Fluid-Dynamic Lift*, Hoerner Fluid Dynamics, Vancouver, WA, 1975, pp. 2.6–2.7.

[7]White, F. M., "Boundary-Layer Flows," *Fluid Mechanics*, 2nd ed., McGraw–Hill, New York, 1986, p. 418.

[8]Gleyzes, C., Cousteix, J., and Bonnet, J. L., "Theoretical and Experimental Study of Low Reynolds Number Transitional Separation Bubbles," *Proceedings of the Conference on Low Reynolds Number Airfoil Aerodynamics*, edited by T. J. Mueller, Springer-Verlag, 1985, pp. 137–152.

[9]Lang, M., Rist, U., and Wagner, S., "Investigations on Disturbance Amplification in a Laminar Separation Bubble by Means of LDA and PIV," *Proceedings of the 11th International Symposium on Applications of Laser Techniques to Fluid Mechanics*, July 2002.

[10]Barlow, J. B., Rae, W. H., and Pope, A., "Boundary Corrections I: Basis and Two-Dimensional Cases," *Low Speed Wind Tunnel Testing*, 3rd ed., Wiley, New York, 1999, pp. 328–366.

[11]"Assessment of Experimental Uncertainty with Application to Wind Tunnel Testing," AIAA Standard S-071A-1999, AIAA, Reston, VA, 1999.

[12]Kwon, K., and Park, S. O, "Aerodynamic Characteristics of an Elliptic Airfoil at Low Reynolds Number," AIAA Paper 2005-4762, June 2005.

[13]Abbott, I. H., and von Doenhoff, A. E., "Aerodynamic Characteristics of Wing Sections," *Theory of Wing Sections—Including a Summary of Airfoil Data*, Dover Publ., Inc., New York, 1959, pp. 462, 463.